CONF-9010212--2
Recd.

CONF-9010212--23

DE91 004768

# Simulation Studies for Design Optimisation of a Scintillator Plate Calorimeter

Jim Proudfoot†, P. K. Job, and H.-J. Trost
Argonne National Laboratory
T. Handler, University of Tennessee
T. A. Gabriel, Oak Ridge National Laboratory

Paper presented at the
Symposium on Detector Research and Development
for the Superconducting Super Collider
October 15 - 18, 1990
Ft. Worth, Texas



**Prepared by the**
**OAK RIDGE NATIONAL LABORATORY**
**Oak Ridge, Tennessee 37831**
**managed by**
**MARTIN MARIETTA ENERGY SYSTEMS, INC.**
**for the**
**U.S. DEPARTMENT OF ENERGY**
**under contract DE-AC05-84OR21400**



† Managed by Martin Marietta Energy Systems, Inc. under Contract No. DE-AC05-84OR21400 for the U.S. Department of Energy.

# SIMULATION STUDIES FOR DESIGN OPTIMISATION OF A SCINTILLATOR PLATE CALORIMETER+

Worthington Hotel
Forth Worth, Texas
October 15-18, 1990

J. Proudfoot, P. K. Job, H.-J. Trost
Argonne National Laboratory

T. Handler
University of Tennessee

T. Gabriel
Oak Ridge National Laboratory

Presented by James Proudfoot
High Energy Physics Division, Argonne National Laboratory
9700 South Cass Avenue, Argonne, Illinois 60439

## Abstract

Results on simulations studies relating to the optimisation of a sampling scintillator plate calorimeter for an SSC detector system are presented. These studies show that whereas a compensating sampling geometry can be obtained using a variety of configurations using either lead or depleted uranium as the principal absorber, no configuration based on a pure iron absorber is compensating. Unlike in a lead system, delayed energy release from long lived shower products produced in a uranium system pose a serious pile up problem. Therefore we advocate the use of lead as the principal absorber in this calorimeter. Work on optimisation of the mechanical structure is in progress and results are presented on issues such as structural support, tolerances and on the degradation in response due to other detector material within the volume of the calorimeter.

## Introduction

The detector designers of experiments at the SSC have the task of determining the most effective means of achieving high performance physics measurements in the distinctly hostile radiation field from the hadron collisions themselves. To further increase the difficulty of this task such a detector must be designed in the next few years, fabricated in a timely fashion to allow installation by beam turn on at the end of the decade and then yield physics measurements for many years thereafter. For a detector component such as the calorimeter, major refurbishment is unimaginable and therefore this detector must be designed for the maximum luminosity lifetime anticipated (an ill defined target since it depends on actual physics results). This varies from a lifetime of ten years at a luminosity of $10^{33}$ cm$^{-2}$ s$^{-1}$ to $10^{34}$ cm$^{-2}$s$^{-1}$.

The use of sophisticated simulation programs to evaluate calorimeter performance is now commonplace. Over the last ten years, the models and approximations embedded in such programs have been well tested and the use of EGS (1) to simulate electromagnetic response, CALOR (2,3) to simulate hadronic response and GEANT (4) to simulate the physics response is expected to give reliable predictions of detector performance. The talks presented

The scintillator saturation constant (Birk's Constant) was assumed to be 0.0131, which is typical of scintillators under consideration.

The parameter space used for the subsequent three absorbers was:

- Absorber composition (pure lead, iron, and depleted uranium).
- Absorber thickness
- Scintillator thickness
- Signal integration gate
- Energy deposition time profile

The e/h ratio as a function of absorber thickness for a constant scintillator thickness of 0.25 cm and an integration gate of 48 nsec is shown in Fig. 2. Both lead and uranium systems allow a geometry yielding e/h = 1. This is not the case for the iron system. The calculations are seen to be in good agreement with the available experimental data (Refs. 5-7).

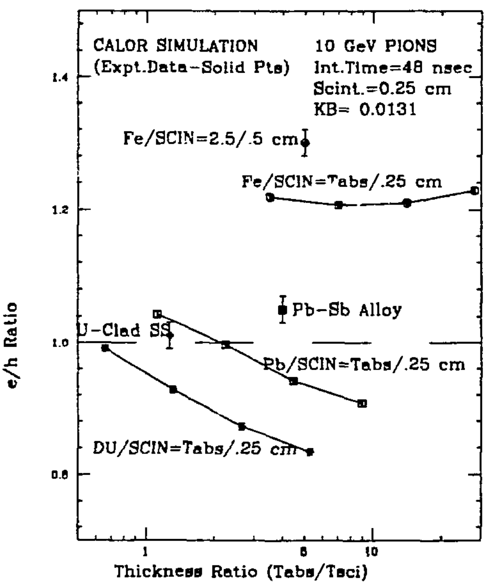


**Figure 2.** Relative response of electrons to pions (e/h) as a function of absorber thickness (Tab) and composition for a fixed scintillator thickness of 0.25 cm. Also shown are experimental data (Refs. 5-7).

Figure 3 shows e/h as a function of pseudorapidity (η) under the assumption of constant plate and scintillator thickness in the compensating uranium/scintillator geometry of 0.33:0.26 cm. Only a modest increase of e/h of around 5% is seen which is emminently acceptable with respect to degradation of the constant term in the resolution. The slope of e/h versus absorber thickness for lead/scintillator is flatter than that for depleted uranium/scintillator (Fig. 2). Therefore, the rapidity variation in the lead system will be comparable to or less than that measured in the uranium/scintillator system. Clearly no rapidity variation is expected in the iron/scintillator system as e/h is computed to be independent of absorber thickness.

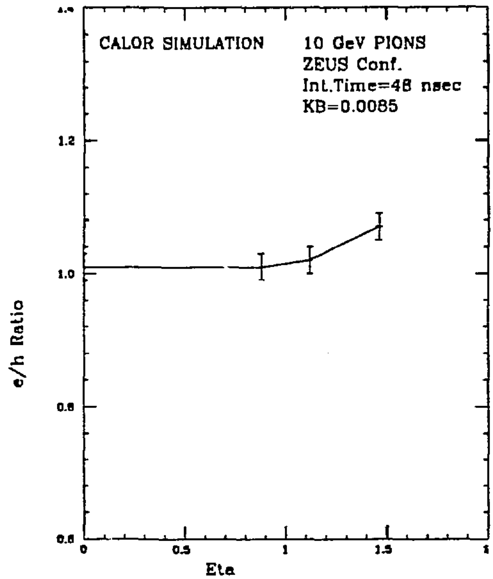


**Figure 3.** e/h as a function of pseudorapidity (η) for the ZEUS compensating uranium geometry having a scintillator thickness of 0.26 cm.

The variation of e/h for fixed absorber thickness is shown in Fig. 4 (again for an integration gate of 48 nsec). This predicts that for a sampling frequency in lead of 1 radiation length, which is characteristic of that required for an electromagnetic calorimeter, a scintillator thickness of 0.25 should yield compensation. This is a key issue in the use of lead as the passive absorber, where fine sampling is required for good resolution and where the nominal 4:1 ratio of absorber to scintillator thickness would seriously compromise the performance of the electromagnetic calorimeter.

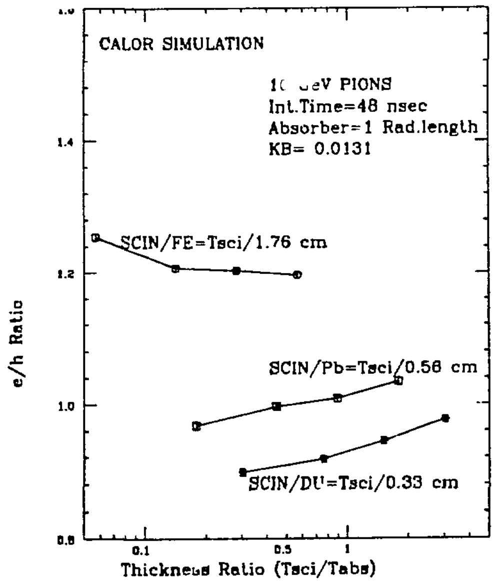


**Figure 4.** e/h as a function of scintillator thickness for a fixed absorber thickness of 1 radiation length.

Finally, the dependence of e/h with integration time is shown in Fig. 5 for the nominal compensating iron, lead and depleted uranium systems. Both lead and depleted uranium systems rapidly achieve e/h ~ 1. However, in the case of depleted uranium, energy from long lived products of the hadron shower continue to be measured up to 500 nsec after the primary shower. These contribute a significant amount of energy (~ 20%) and pose a serious problem with regard to pile up.

Our conclusion from this analysis is that firstly pure iron should be removed from consideration as it does not yield compensation in any configuration. However, this result for iron is a topic of considerable debate and we are currently pursuing studies to determine the possibility of obtaining compensation in a composite iron structure. These results are discussed in more detail in the talk of T. Handler at this conference. An initial study used 2.54 cm thick iron absorber and 1 cm of scintillator segmented into five independent sections. Figure 6 shows e/h as a function of scintillator segment depth in this geometry. Little improvement in e/h is observed. These studies are continuing.

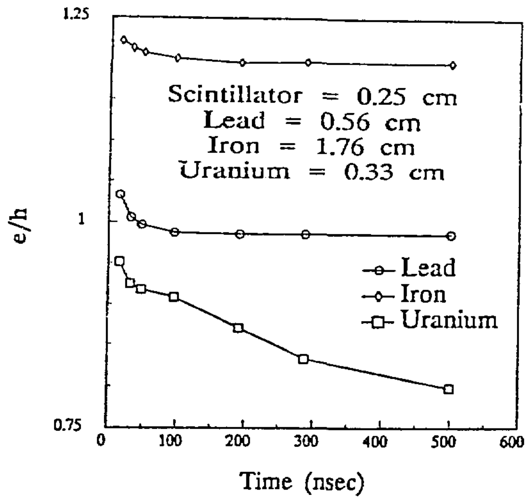


**Figure 5.** e/h for lead, iron and uranium calorimeters with nominal compensating geometries as a function of signal integration time.

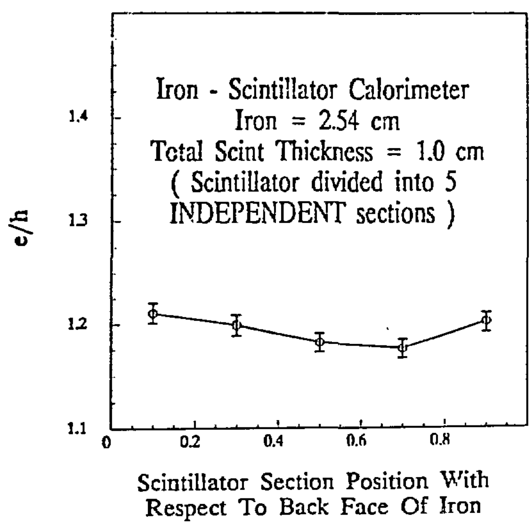


**Figure 6.** e/h as a function of scintillator section position.

Both lead and depleted uranium can yield identical levels of compensation in comparable sampling geometries. As there are finite limits on scintillator plate thickness this results in calorimeters with essentially identical resolutions. Both are relatively insensitive to the rapidity non-uniformity intrinsic to the sampling plate geometry. However, the significant delayed energy release predicted in the uranium system relative to the lead system indicates a potentially serious pile-up problem. (This result must be verified by experiment.) This in addition to other factors such as safety, materials, and fabrication costs results in our advocating the use of lead as the principal absorber in the calorimeter (despite the advantages of calibration and reduced radius associated with the use of depleted uranium). We are therefore proposing to further evaluate the mechanical design of a lead/scintillator calorimeter in FY91.

**Detailed Design Optimisation**

To proceed from the general design outline above which advocates the use of a pure lead calorimeter with 0.5 cm lead plates and 0.25 cm scintillator plates one must include additional constraints. From the mechanical perspective these include:

- Scintillator composition (especially as is required for radhard characteristics.
- Location, size and orientation of structural supports.
- Gap, absorber, and scintillator tolerances and their effect on response uniformity.
- Global mechanical design issues such as flat versus staggered plate geometries.

Furthermore, from the perspective of the calorimeter as a component in a full detector system, these include:

- Transverse cell size
- Longitudinal sampling frequency (and its resulting effect on electromagnetic and hadronic energy resolution
- Depth segmentation (and its effect on e-π separation)
- Impact and correction for detector systems within the inner volume of the solenoid.
- Cost
- Radiation damage effects on uniformity and stability

I will briefly illustrate studies into some of these issues.

**Mechanical Issues**

A commonly neglected variable in compensation studies is the value of Birk's constant (kB), which describes scintillator saturation effects. This is discussed in more detail in the presentation of T. Handler at this conference. The difference

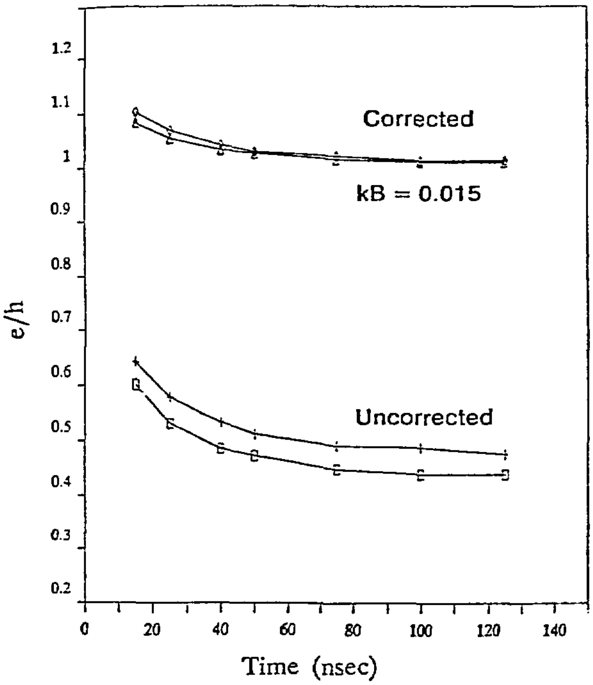


**Figure 7.** e/h in a Pb scintillator calorimeter with 0.56:0.25 cm sampling as a function of neutron cutoff time, assuming kB = 0 and kB = 0.015.

between corrected and uncorrected light yields is shown in Fig. 7 for a lead scintillator system with Pb: scintillator ratio of 0.56:0.25 cm. The effect of saturation of the light yield from low energy particles (including the important proton recoils) is seen to be enormous. At a more realistic level the difference between kB = 0.015 and kB = 0.008, which are values for actual acrylic scintillators, corresponds to a 10% effect in e/h for equivalent systems. The present optimisation assumes kB = 0.0131. Once data on the actual radhard scintillator to be used is available, the design optimisation will be re-iterated.

The support structure for the calorimeter and detectors within are an area of concern as they can result in projective cracks and loss of heremeticity. As an alternative to a strictly radial cut for these supports we have studied the feasibility of using a tower structure which is pseudoprojective in $\eta$ to improve the measurement of signal in the barrel-endplug transition region. This is achieved by projecting the towers at large $\eta$ to a point offset by some distance in z from the true beam crossing point. The minimal response in the barrel-endcap transition region for 10 GeV $\pi^-$ incident as a function of this offset is shown in Fig. 8

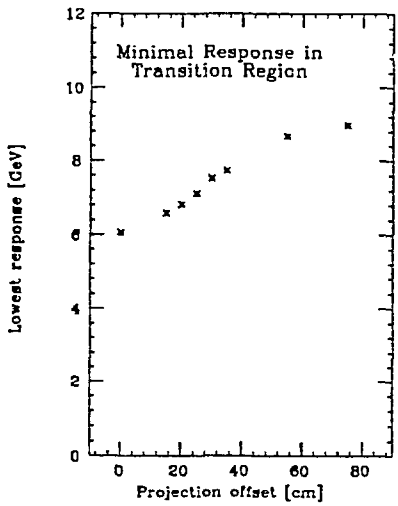


**Figure 8.** Minimal response to 10 GeV $\pi^-$ in the barrel-endplug transition region as a function of projective offset, assuming a 1" aluminum support ring at the boundary.

(where we have assumed a 1" aluminum support ring). It is possible to cover this gap by using a rather modest offset of 60 cm. However, resolution is degraded in this region and the scale of this degradation is sensitive to the size of the physical gap required for cables and support services. As a result our collaboration decided to retain a true endcap design as the more conservative choice for a sampling plate calorimeter (the alternative is still a viable option however for this or other technologies).

Another issue for the mechanical design, in particular for a lead calori meter, is that of thickness tolerance. Lead is well known to creep, to be difficult to roll flat and in the option of a cast lead fabrication liable to shrink during molding. This was judged to be principally an issue for the electromagnetic calorimeter and was studied using EGS in a detector whose nominal sampling was 30 layers of 0.5 cm Pb and 0.25 cm scintillator. The absorber thicknesses were varied randomly in a window of 0, ± 5, 10, and 20% from the nominal thickness and the resulting calorimeters surveyed with electrons of energy 1, 2.5, 5.0, 10.0, and 25 GeV. The samples were chosen to yield approximately identical statistical errors on the mean responses for all energies. The overall performance was computed as the average response in MeV (deposited)/ GeV (incident energy) over the five beam energies. The resulting comparison of average deposited energy with respect to a perfect calorimeter as a function of absorber thickness tolerance is shown in Fig. 9. A systematic change in response is observed due to the dispersion of the EM shower profile. For a simple system in which plates are flat but of varying thickness, in situ calibration can correct this mismatch for electron showers. This however is not wholly the case for either non-flat plates or for hadron showers. The data show that to maintain a constant

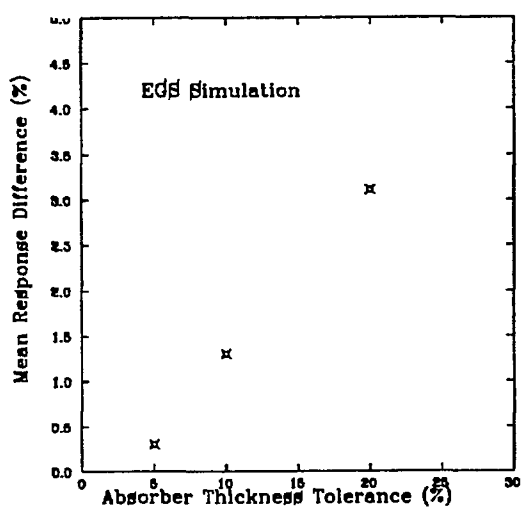


**Figure 9.** Difference in scintillator energy deposition averaged over incident electron energies of 1, 2.5, 5.0, 10.0, 25.0 GeV wrt perfect absorber thickness of 0.5 cm for 0.5:0.25 cm ratio Pb:Scint.

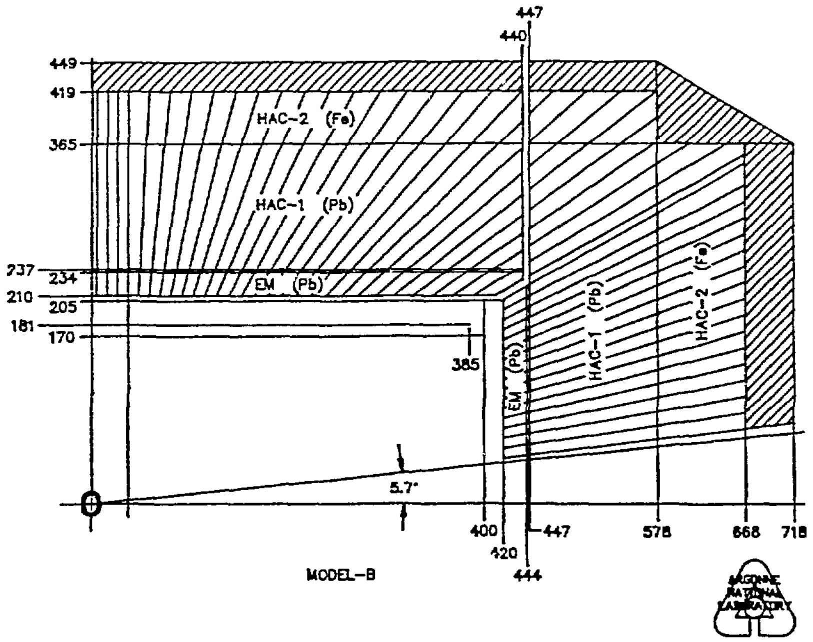


Figure 10. Conceptual design layout for the SDC detector showing one electromagnetic, and two hadronic calorimeter compartments.

term in the resolution of ≤ 1% the absorber thickness tolerance must be maintained to within 8% for 0.5 cm nominal absorber sampling. This is not anticipated to be a limitation on the casting approach currently advocated by the scintillator plate collaboration for lead electromagnetic and hadronic calorimeters.

Other issues for the mechanical design such as the difference between staggered and flat plate geometries (as advocated for an iron calorimeter and as may be demanded for mechanical reasons in a lead-composite calorimeter) are currently under study. Preliminary results show that although the staggered plate geometry may yield superior hadron resolution it may also contribute to a significant constant term. Our current position is to proceed with a flat plate design for both electromagnetic and hadronic calorimeters.

**Detector Issues**

The detector within whose context this calorimeter design is being carried out is shown in Fig. 10. Topics of hot debate in this design are those of transverse and longitudinal granularity. A GEANT calculation of the lateral shower profile for 10 GeV pions is shown in Fig. 11. The significant characteristic is that 65% of the shower is contained within a projective tower subtending 10 × 10 $cm^2$ at a

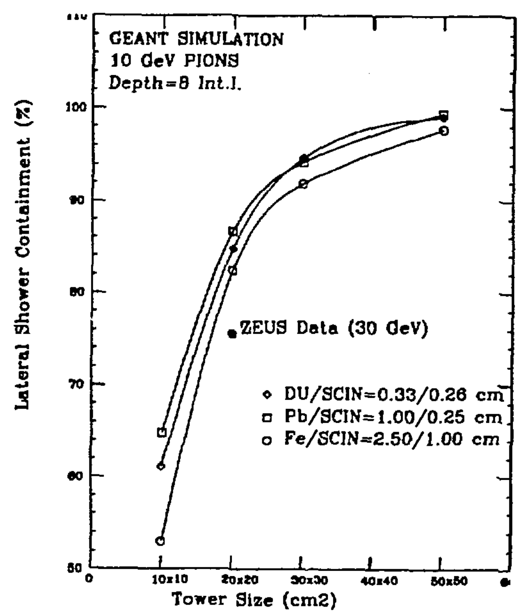


Figure 11. Lateral shower profile for 10 GeV pions incident on projective calorimeter towers.

radius of 2m from the interaction point (note that this conclusion is approximately independent of absorber medium). Therefore, transverse granularity finer than 10 × 10 $cm^2$ only increases the sensitivity to the single particle shower profile. As this is of no import in a jet environment we advocated (and adopted) the angular cell size of 10 × 10 $cm^2$ at a 2m radius and 90° to the beam.

As is indicated in Fig. 10, three depth measurements of the energy deposition are envisaged. The first segment is for use in identification of electrons and photons by longitudinal shower development. Current knowledge states that to maximise e/π separation this should be roughly 25 $X_0$ by maximising the containment of electromagnetic showers for a minimum number of hadron interaction lengths. GEANT simulations of the optimum geometry and the effect of increased absorber with η are in progress. In the cast lead fabrication approach there is reduced flexibility in the choice of absorber geometry at high η coming from mechanical limitations and these studies will be used to determine the optimal working point.

The outer calorimeter compartment is currently considered to be required to return magnetic flux and is therefore iron (and hence allowing less than perfect compensation). In this design, therefore, the intermediate section comprises the high resolution compensating hadron calorimeter. The depth of this section is therefore crucial to the overall linearity of the calorimeter. The energy deposition from neutrons in a compensating Pb/scintillator calorimeter is shown in Fig. 12 for 10 GeV $\pi^-$ incident. 90% of the neutron energy is contained within 4.3 interaction lengths of absorber. This result can be extrapolated to high energy hadron showers by appealing to existing experimental data (Ref.8). These data indicate that hadron shower maximum moves approximately 0.6 interaction lengths deeper into a Pb stack as the incident pion energy increases from 10 to 100 GeV. Therefore, a minimum of 5 interaction lengths is required to contain 90% of the neutron energy deposition from a 100 GeV pion. In the above configuration, the iron calorimeter would thus mismeasure the pion energy by 0.2% due to mismeasurment of the neutron component. This is an acceptable

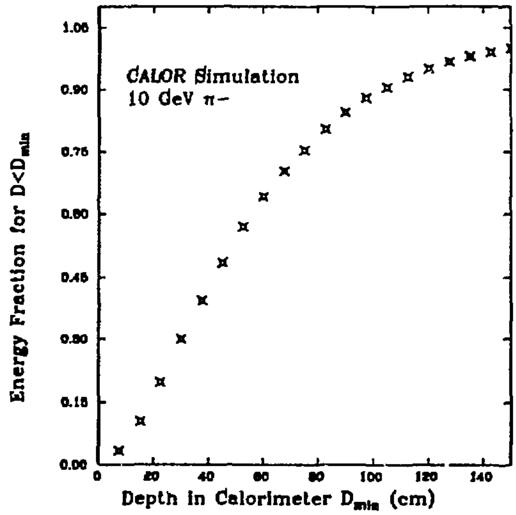


Figure 12. Fraction of energy deposited in scintillator by neutrons as a function of depth in a lead calorimeter with unit cell 0.56:0.25 Pb:Scintillator

compromise with respect to the constraints of outer radius and magnetic flux return.

The final issue I shall discuss in this presentation is that of the coil required to generate the solenoidal field in this detector. This contributes a thickness of aluminum of around 1.1 $X_0$ distributed at lumped radii over 35 cm in total radius. It therefore, smears electromagnetic showers by absorption of low energy electrons and by allowing showers initiated in the coil to propagate in vacuum. This effect is largest at maximum angle of incidence, which is roughly 25° to the beam in the detector under consideration. This is illustrated in Fig. 13, where a Pb calorimeter with its first layer being 0.5 cm Pb (and no coil) is compared with one having its first layer being 0.25 cm scintillator with a simulated coil and front plate as the first absorber. This cell geometry is sketched in Fig. 14. Considerable nonlinearity is predicted (with corresponding

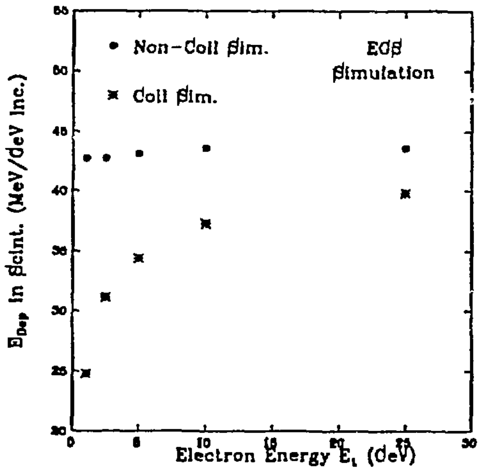


**Figure 13.** Calorimeter response at 25 degree incident angle as a function of energy for the case of a perfect calorimeter and one including material to simulate a solenoid coil.

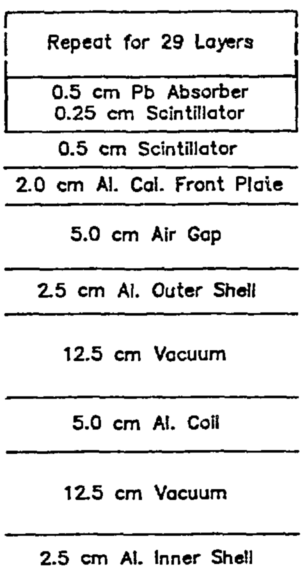


**Figure 14.** Material distribution for coil simulation studies on calorimeter performance for configuration using double sampling in the first scintillator layer.

detrimental effects being seen in the resolution. Studies are now in progress to utilise modification of the scintillator thickness and sampling distribution to reduce this effect. These are shown in Fig. 15 for the unmodified sampling configuration and two initial candidate geometries:

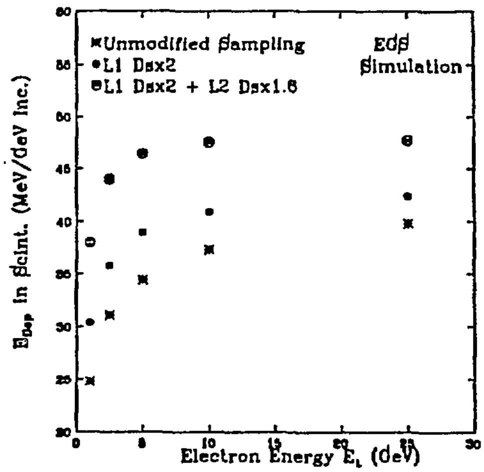


**Figure 15.** Calorimeter response at 25 degree incident angle with coil simulation and modified sampling distributions as described in text.

a) L1 Ds x 2, in which the first scintillator layer thickness is doubled to 0.5 cm.
b) L1 Ds x 2 + L2 Ds x 1.6, in which in addition to doubling the thickness of the first scintillator layer, the thickness of the second layer is increased by 1.6.

Considerable improvement is observed in the linearity and in the energy resolution, which is shown in Fig. 16. However, much work remains to be done to optimise the overall geometry for electron energy measurement within the constraint of retaining e/h close to 1.

## Conclusions

We have shown that a high resolution compensating calorimeter can be built using either lead or depleted uranium as the principal absorber. Studies to date indicate that this is not possible, even with some composite tuning, in an iron based calorimeter. Energy release from long lived shower products contributes a significant fraction of the shower energy in a uranium calorimeter for times up to 500 nsec after the collision. We therefore, judge that for this reason that lead should be used as the principal absorber.

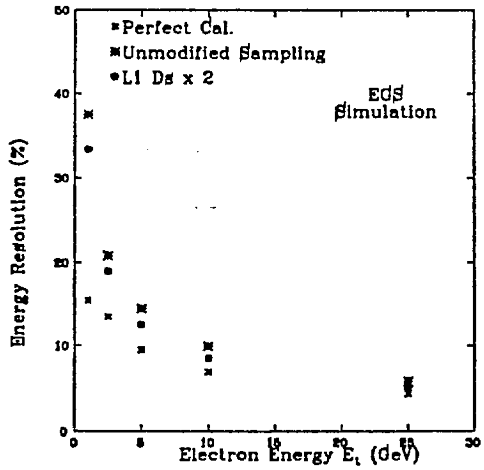


**Figure 16.** Calorimeter resolution at 25 degrees incident angle for perfect, coil simulation and modified sampling distributions as described in the text.

Detailed mechanical design studies of a lead-composite calorimeter have begun. Radial and pseudo-projective barrel-endcap transitions in which support structure for the barrel calorimeter and coil is located have been evaluated. Both are viable. However, it is our opinion that the more conservative design to use is that of a radial cut. The casting technology anticipated for the fabrication of this calorimeter can be anticipated to yield non-uniform absorber thickness due to shrinkage. Our studies show that this predominantly effects the constant term in the resolution of the electromagnetic calorimeter. This can be held to < 1% by maintaining an absorber thickness tolerance of better than ± 8%, which is far worse than the expected tolerance. The detector design requires magnetic flux return and therefore an iron calorimeter segment at the outer radius (to minimize the overall radius). We have studied the longitudinal energy deposition from neutrons in a lead calorimeter system and conclude that this section should have a depth of at least 6.9 absorption lengths to yield an acceptable mismeasurement of 100 GeV pions. Much more work, however, is needed to evaluate the effect of the non-uniform sampling distribution on the constant term in the resolution for hadron showers. Other issues requiring further study include material alloys and internal support structure.

Finally, the coil of the solenoid required in the detector is a necesary evil. As is now well known, "massless gaps" can compensate for energy loss and smearing in the coil and thereby improve linearity and resolution. Studies are in progress and show severe degradation in performance at the outer ends of the barrel calorimeter. Much more work is needed in this area to properly compensate this degradation.

---

+ Work supported in part by the U.S. Department of Energy, Division of High Energy Physics, Contract W-31-109-ENG-38.

### References

[1] W. R. Nelson, H. Hirayama and D. W. O. Rogers, EGS4 Code System, SLAC 265 (1985).

[2] T. W. Armstrong and K. C. Chandler, HETC - A High Energy Transport Code, Nucl. Sci. and Eng. 49, 110 (1972).

[3] Monte Carlo High Energy Nucleon-Meson Transport Code, ORNL RSIC Computer Code Collection, CCC-178.

[4] R. Brun, F. Brayant, M. Maire, A. C. McPherson and P. Zanarini, GEANT3 Users Guide, CERN Report DD/EE/84-1 (1986).

[5] H. Abrahamowicz et al., The Response and Resolution of an Iron-Scintillator Calorimeter for Hadronic and Electromagnetic Showers Between 10 GeV and 140 GeV, Nucl. Inst. Meth. 180, 429 (1980).

[6] E. Bernadi et al., Nucl. Inst. Meth. A262, 229 (1987).

[7] E. Ros and T. Tsurugai, ZEUS Note 88-086 (1988).

[8] W. J. Womersley et al., Nucl. Inst. Meth. A267, 49 (1988).